

Update of the JMA's One-month Ensemble Prediction System

Japan Meteorological Agency, Climate Prediction Division

Atsushi Minami, Masayuki Hirai, Akihiko Shimpo, Yuhei Takaya, Kengo Miyaoka, Hitoshi Sato, Hiroyuki Sugimoto, Ryoji Nagasawa, Satoko Matsueda and Chihiro Matsukawa

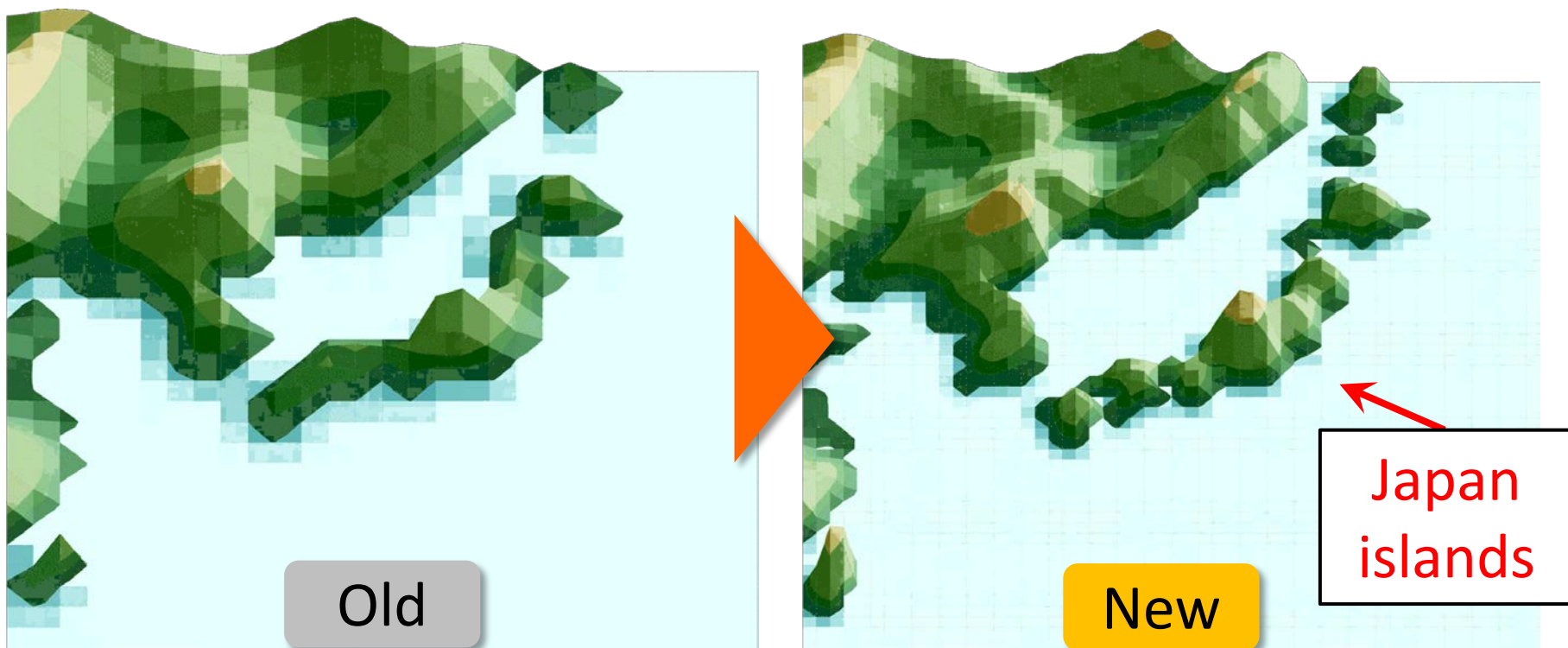


➤ About update of the system

- In March 2014, JMA's One-month Ensemble Prediction System (one-month EPS) was updated.

		Old system	New system
Numerical model		JMA-GSM (<u>Atmospheric General Circulation Model</u>)	
Dx, Dz		Approx. 110km, L60 (Top: 0.1hPa)	Approx. 55km , L60 (Top: 0.1hPa)
Initial condition	Atmosphere	Analysis of global atmosphere	
	Land	Land surface analysis	
Lateral boundary condition	SST	Persisted anomaly (1° × 1°)	Persisted anomaly (<u>0.25° × 0.25°</u>)
	ICE	Climatology	<u>Statistically estimated using initial anomaly with climatological variation</u>
Ensemble size		50 members (25members × 2 initials)	
Perturbation method		Breeding Growing Mode (BGM), Lagged Average Forecast (LAF)	BGM, LAF, and <u>stochastic physics scheme (Buizza et al. 1999)</u>

➤ Increased horizontal resolution



Comparison of the topography used in each system.

- Improvement of the prediction skills such as high frequency eddy activities, blocking are expected owing to the increased horizontal resolution of AGCM (Jung et al. 2012) .
- We confirmed these improvements in the new system.

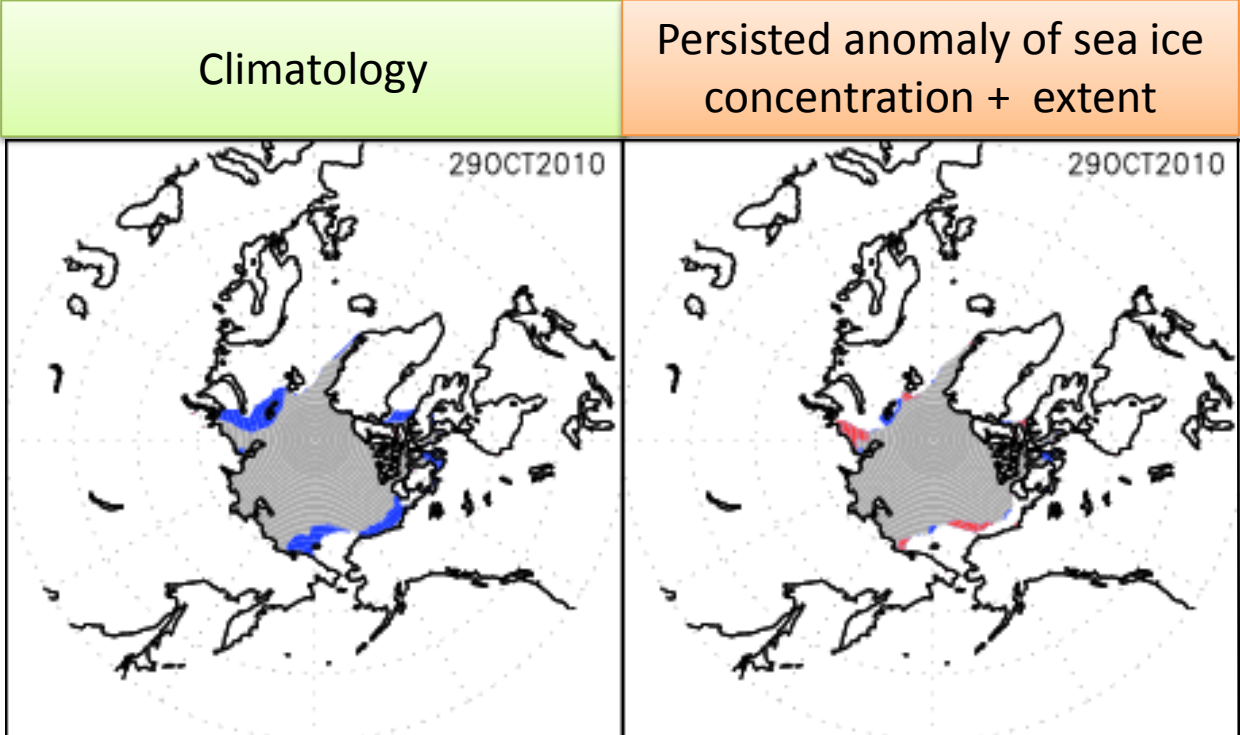
➤ A method of predicting sea ice distribution

- Initial anomalies of sea ice distribution was considered to estimate the distribution more accurately.

~14 days prediction -> Persisted initial anomaly of sea ice concentration

15 days prediction ~ -> Persisted initial anomaly of sea ice extent

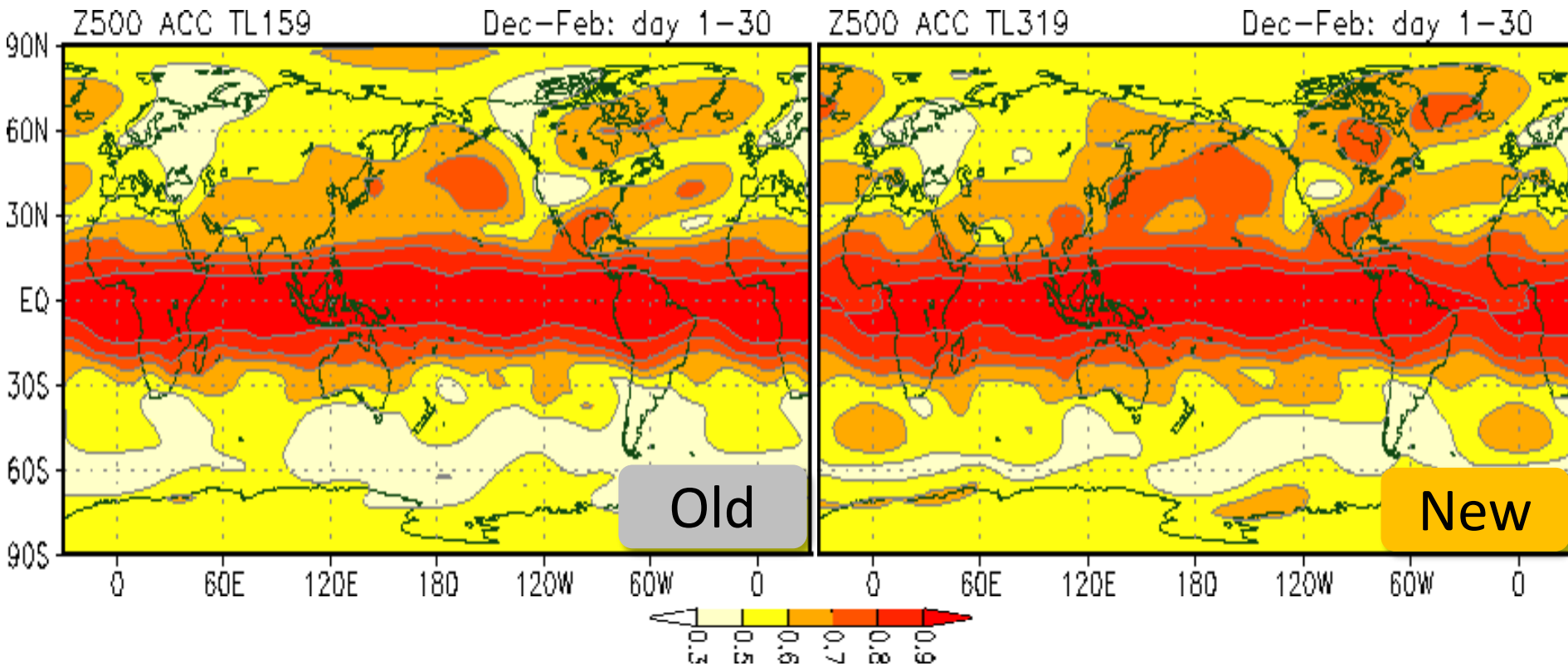
Sea ice distribution	Anl, T	Anl, F
Est, T	grey	blue
Est, F	red	white



WGNE Blue Book
(Sugimoto and Takaya 2013)

- 01Oct2010 initial, 28 days prediction.

➤ Performance of the new system



Comparison of the Anomaly Correlation Coefficient (ACC) of Geopotential height at 500 hPa (Z500) in boreal winter (DJF) . Shading shows ACC of Z500 for 30-day averaged prediction.

- Performance of the new system was evaluated by the hindcast experiment (5member, calculation period is 1981 to 2010) .
- Forecast skills including ACC of Z500 were improved significantly (especially in the extratropical region) .

➤ Change of the product dissemination timing

● Improvement of the prediction skill was large enough to change the dissemination timing of products without loss of prediction skills.

– JMA's One-month EPS products are released every Thursday (a day earlier than before) since March 2014.

The screenshot shows the Tokyo Climate Center website. At the top left is the JMA logo (気象庁 Japan Meteorological Agency). The header includes 'Tokyo Climate Center' and 'WMO Regional Climate Center in RA II (Asia)'. A navigation bar contains tabs for 'Home', 'World Climate', 'Climate System Monitoring', 'El Niño Monitoring', 'NWP Model Prediction' (highlighted with a red box), 'Global Warming', and 'Climate in Japan'. Below the navigation bar, the 'What's New' section lists several updates with dates and 'NEW' tags, such as '16 October 2014 NEW' and '10 October 2014 NEW'. A red arrow points from a blue box in the bottom right corner to the 'NWP Model Prediction' tab. The blue box contains the text 'TCC Website' and the URL 'http://ds.data.jma.go.jp/tcc/tcc/index.html'.

TCC Website
<http://ds.data.jma.go.jp/tcc/tcc/index.html>

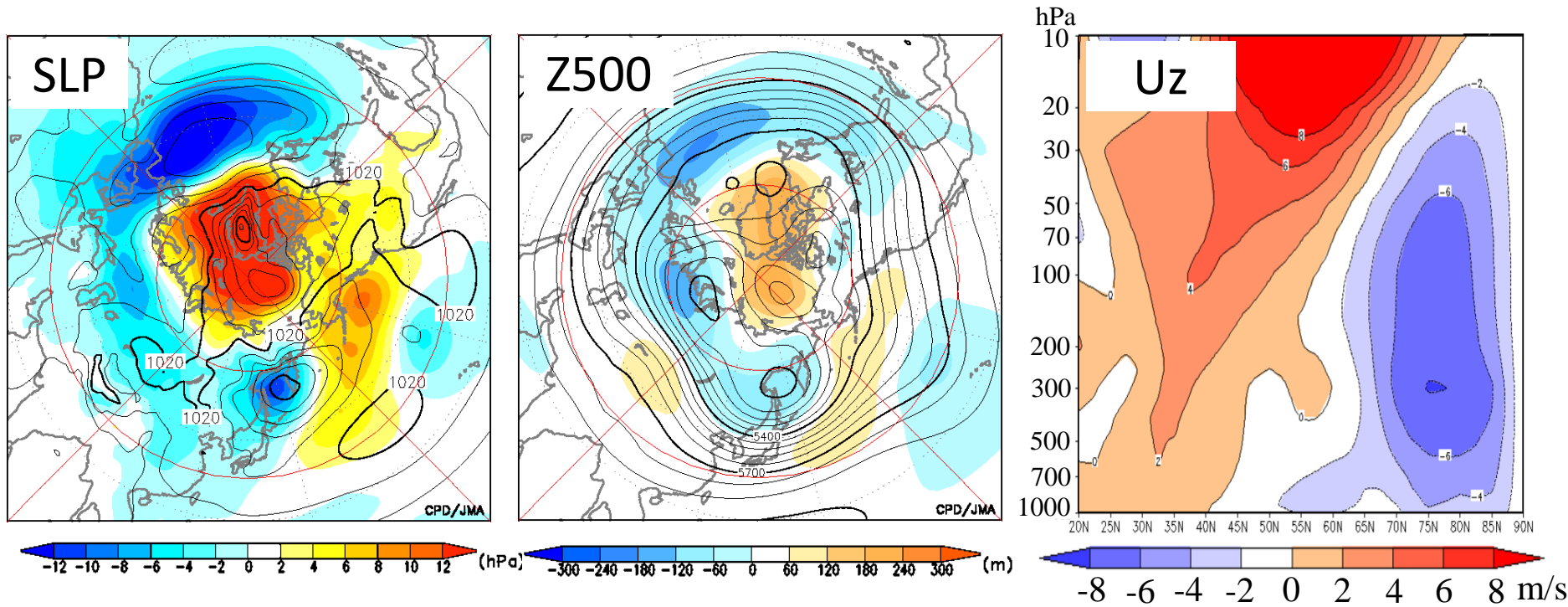
Subseasonal Predictability in negative phases of the Arctic Oscillation

Japan Meteorological Agency, Climate Prediction Division

Atsushi Minami, Yuhei Takaya



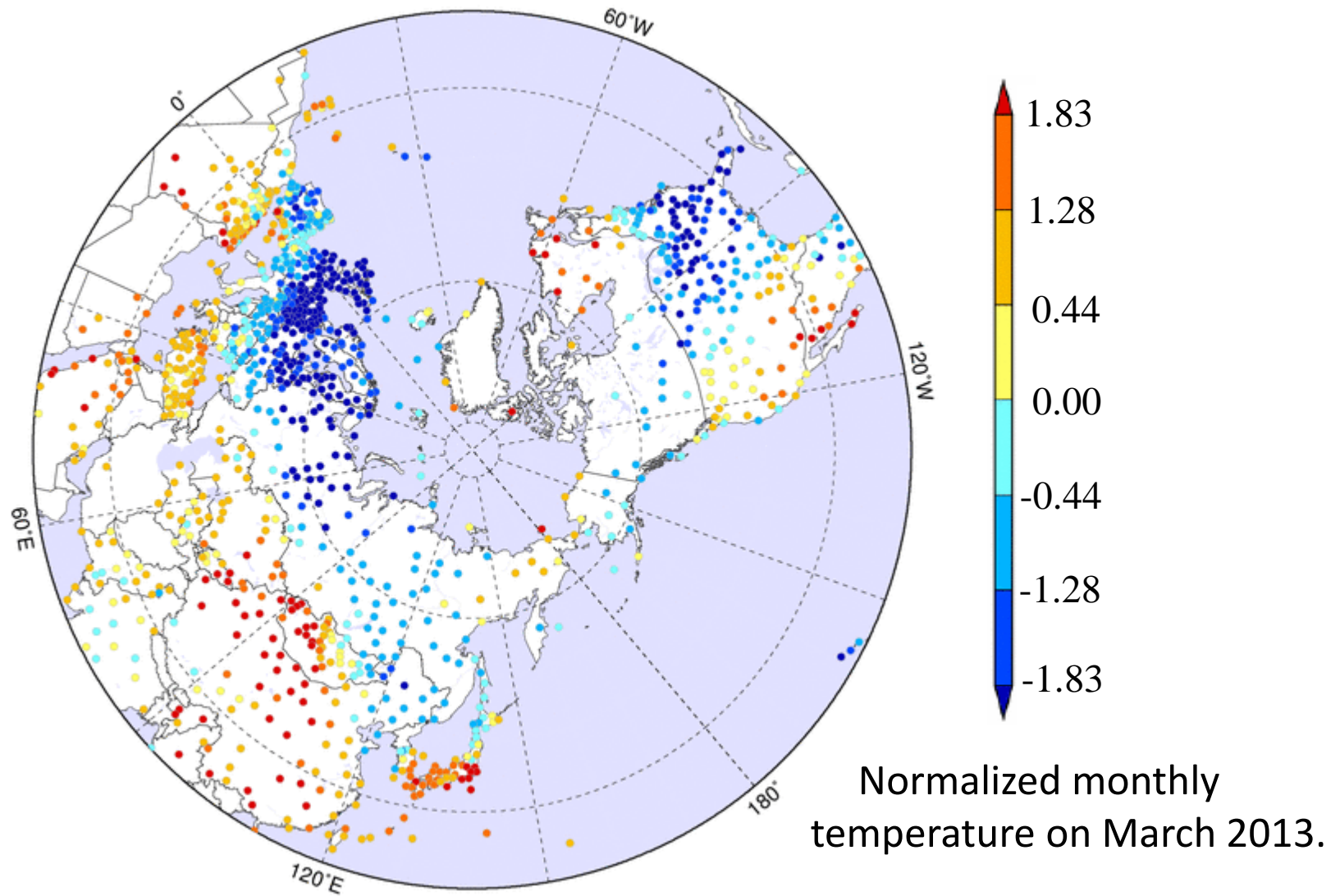
1.1 Arctic Oscillation (AO)



Monthly averaged Sea Level Pressure (SLP) , Geopotential height at 500 hPa (Z500) , Zonal mean wind anomaly (Uz) in the case of March 2013. Shading shows anomaly.

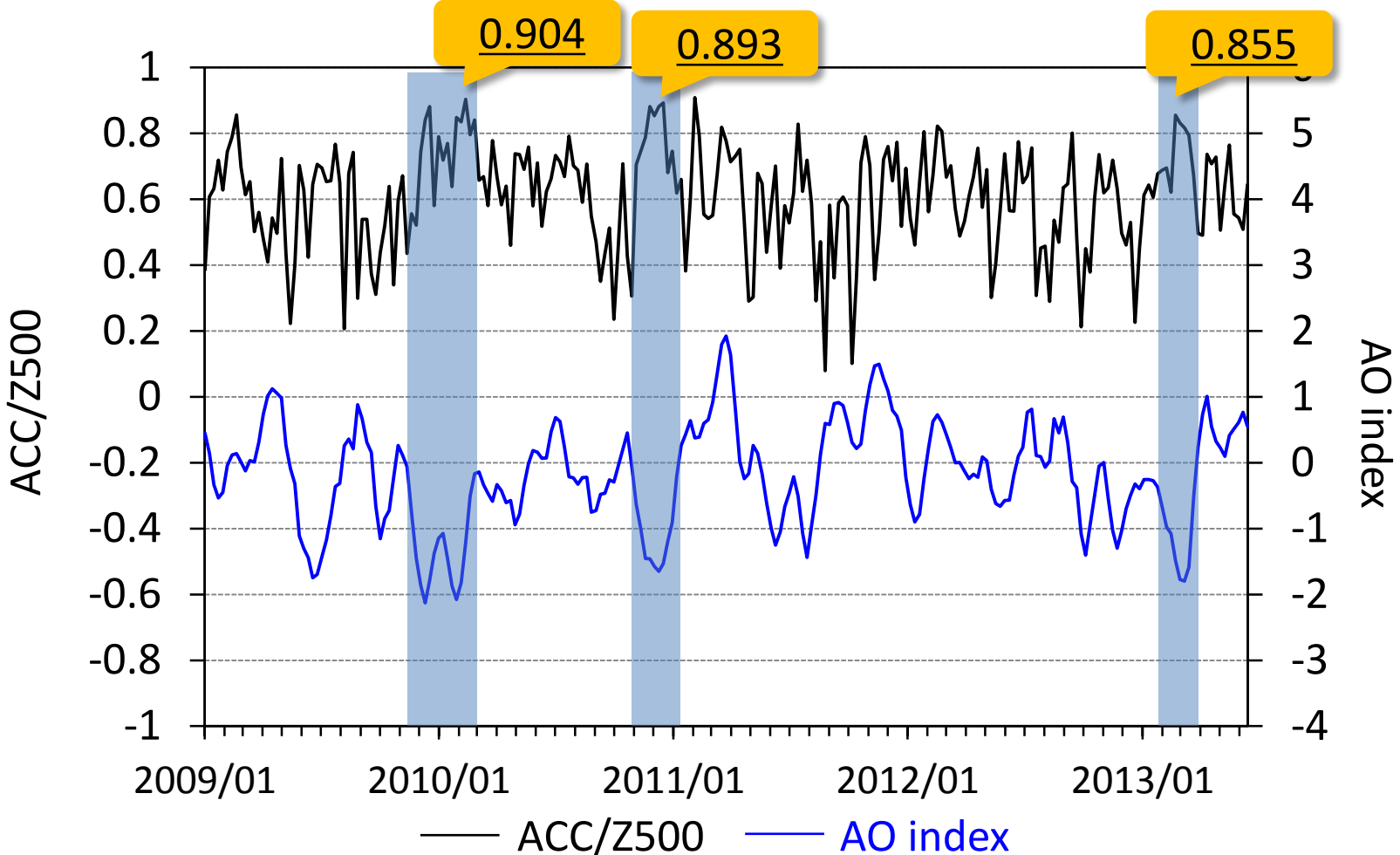
- AO is a leading atmospheric variability in Northern hemisphere (Thompson and Wallace, 1998) .
- The characteristic of AO is the annular pattern of SLP or geopotential anomaly field or meridional shift of westerly jet.

1.2 AO and the temperature in the N.H.



- Negative phase of the AO sometimes result in extreme cold conditions over the hemispheric regions.

1.3 Relationship between AO and prediction skills



The relationship between AO and prediction skill. ACC of 28-day averaged prediction is shown.

- Are negative phases of the AO events predicted well in subseasonal time scale?

1.4 Motivations

- This study aims to address:
 1. The relationship between AO and predictability in subseasonal time scale.
 2. The dynamical processes behind predictability.

using hindcasts of the JMA's operational One-month Ensemble Prediction System (One-month EPS) .

2.1 Data

- Hindcast dataset of the latest JMA's One-month EPS
- JRA-55 (Kobayashi et al., 2015) was used as a verification data
- To focus on the AO in boreal winter, 12 initial dates from 20 Nov. to 10 Mar. with roughly 10-day intervals were used. Total number of initial date used in this study is 360.

Details of the hindcast experiment

Model	Latest JMA AGCM (Ver:1304)
Dx, Dz	About 55km, 60 (top: 0.1hPa)
Ensemble size	5 members
Initial data conditions	JRA-55 (Kobayashi et al., 2015)
SST	Persisted anomaly
Perturbation method	Breeding Growing Mode Stochastic physics scheme (Buizza et al., 1999)
Period	1981 – 2010 (3 initial dates a month)

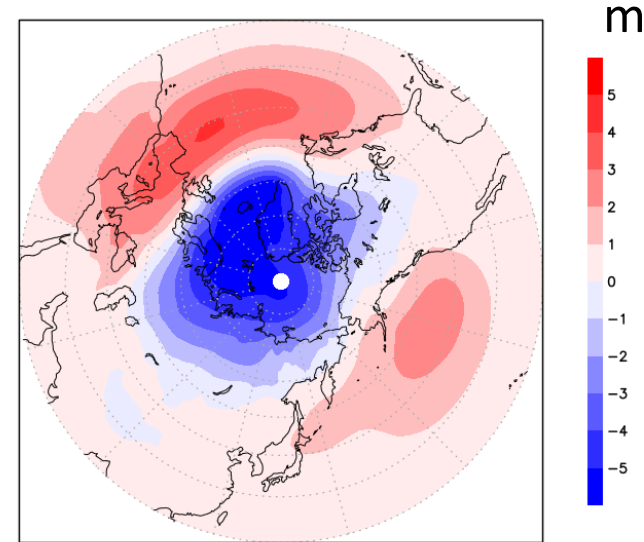
2.2 Method

1. Calculating AO index

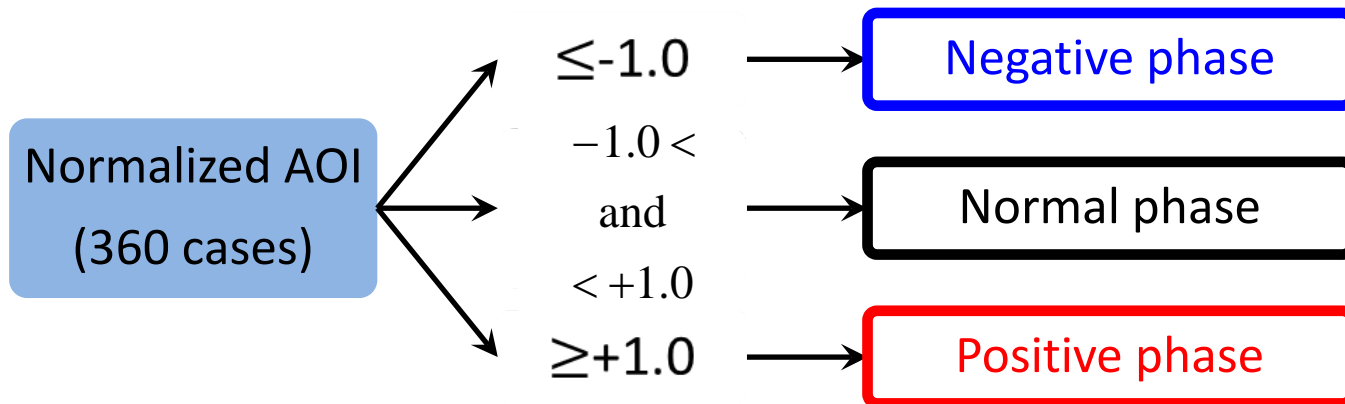
by projecting daily sea level pressure (SLP) fields to the first leading mode of Empirical Orthogonal Function analysis of monthly SLP from December to March of 1981 to 2010.

2. Defining the phase of AO according to the definition below.

3. Investigating prediction skills initiated in the different phases of AO.

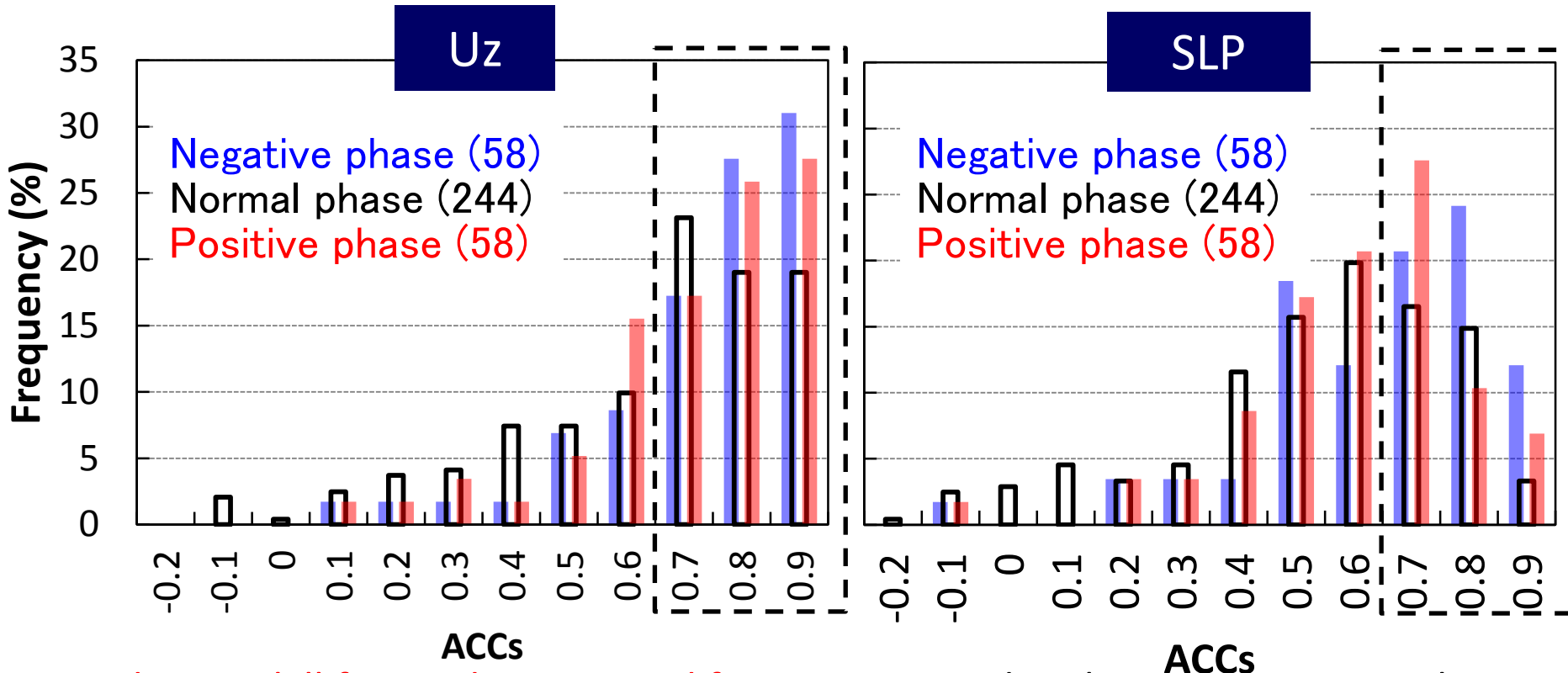


Eigenvector used to calculate AO index.



Definition of the phases of AO

3.1 Prediction skill for each phase event

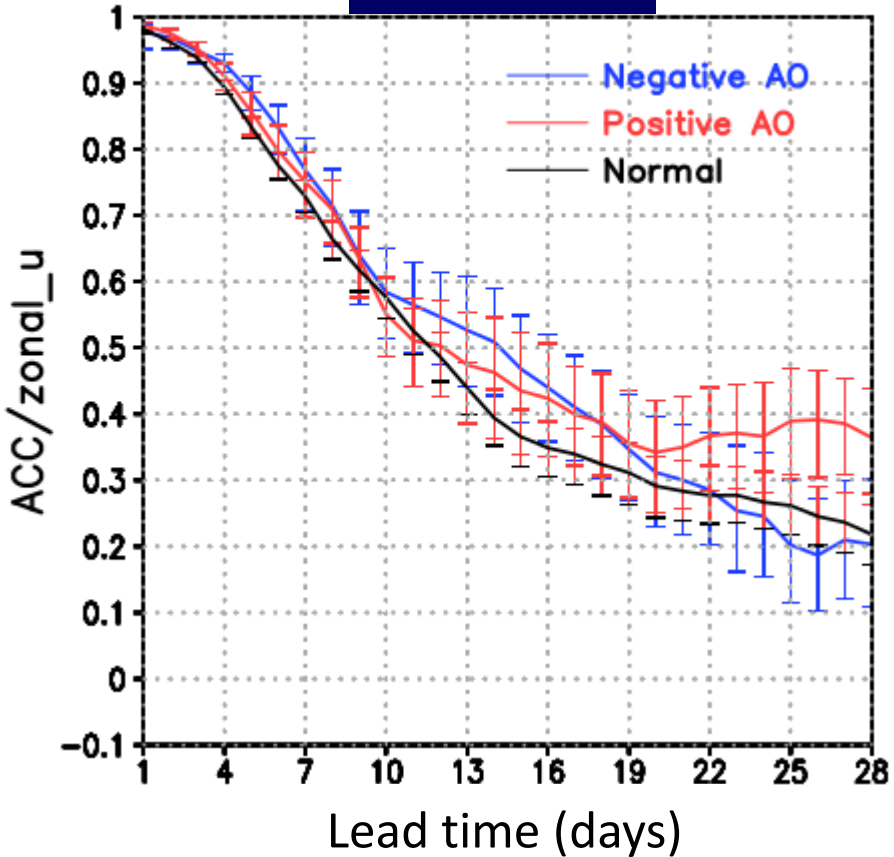


Prediction skill for 28-day averaged forecast initiated in the negative, normal and positive phases of the AO.

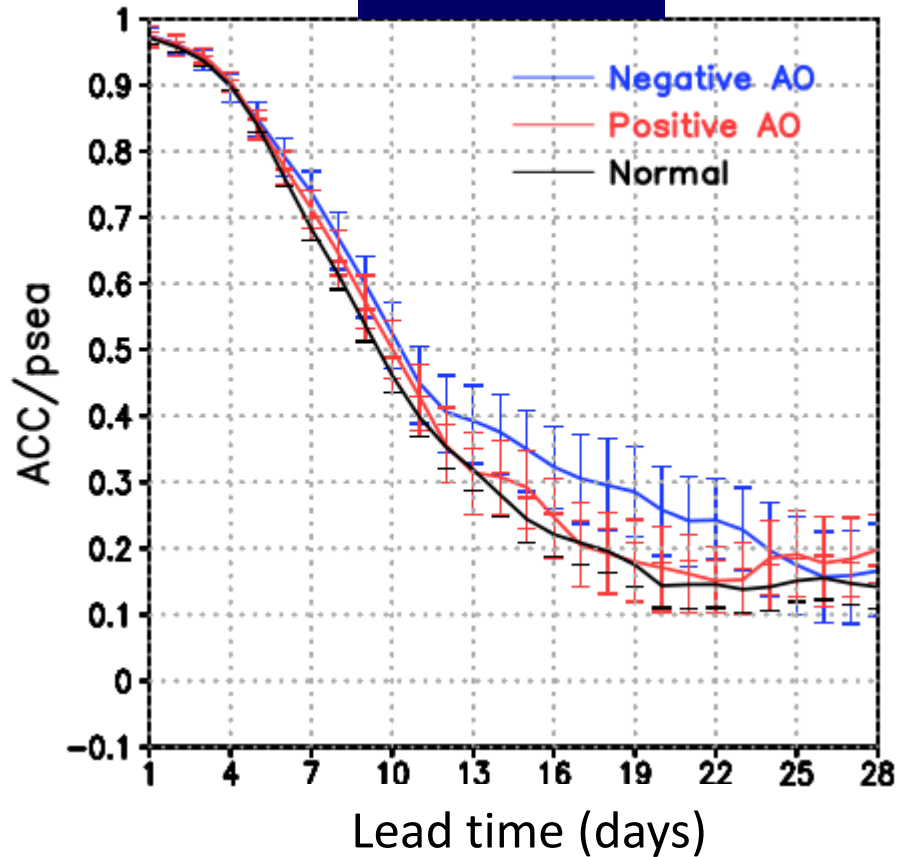
- Negative phase events tend to record higher prediction skills than normal phase as well as positive phase events.
- A ratio of ACCs above 0.7 for SLP (Uz) in negative phases is roughly 25% (15%) higher than that for normal phases.

3.2 Prediction skill for each lead time

ACCs/Uz



ACCs/SLP



Error bar shows the 95% confidence level calculated by 1000 subsamples generated with the bootstrap method.

- ACCs initiated in the negative phases are higher than that in normal phases until about 3 weeks beyond.

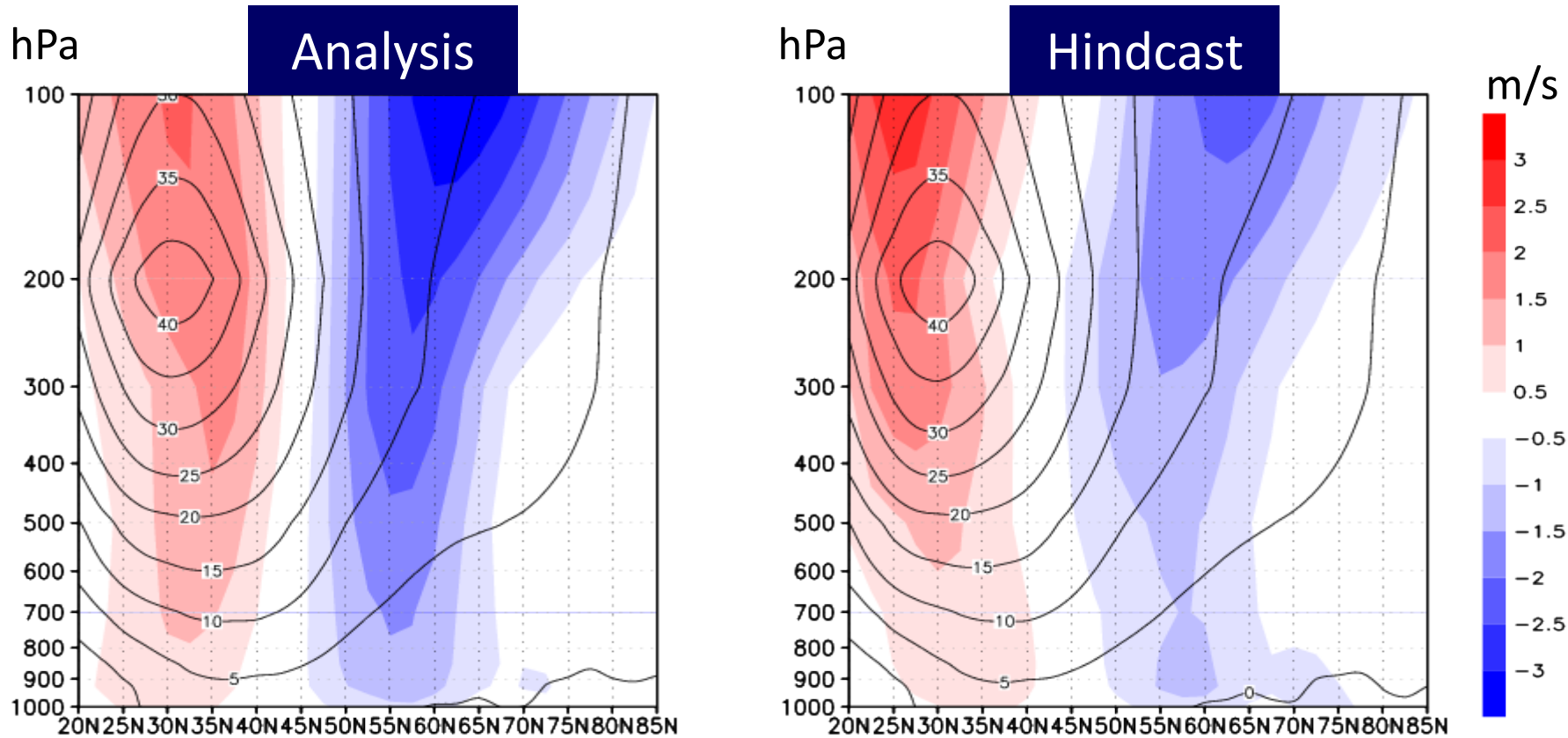
3.3 Dynamical process behind predictability of AO

- Eddies and zonal mean wind interaction is thought to be the basic dynamics for AO variability. This interaction maintains the zonal mean wind anomaly associated AO (e.g. Lorenz and Hartmann 2003) .
 - ⊗ Though stratosphere, ENSO and MJO are also said to be important for AO variability, we focus on tropospheric dynamics here.
- We focused on this dynamical process and analyzed the fields by using Eliassen-Parm flux F (EP flux) .

$$F = \left(-\overline{u'v'}, fR \frac{\overline{v'T'}}{S} \right)$$

- ⊗ Here, u', v' indicate horizontal and meridional wind deviation from each zonal mean respectively and T' is the temperature deviation from the zonal mean. f is coriolis parameter, R is the gas constant and S is static stability. Over bar indicate the zonal mean.

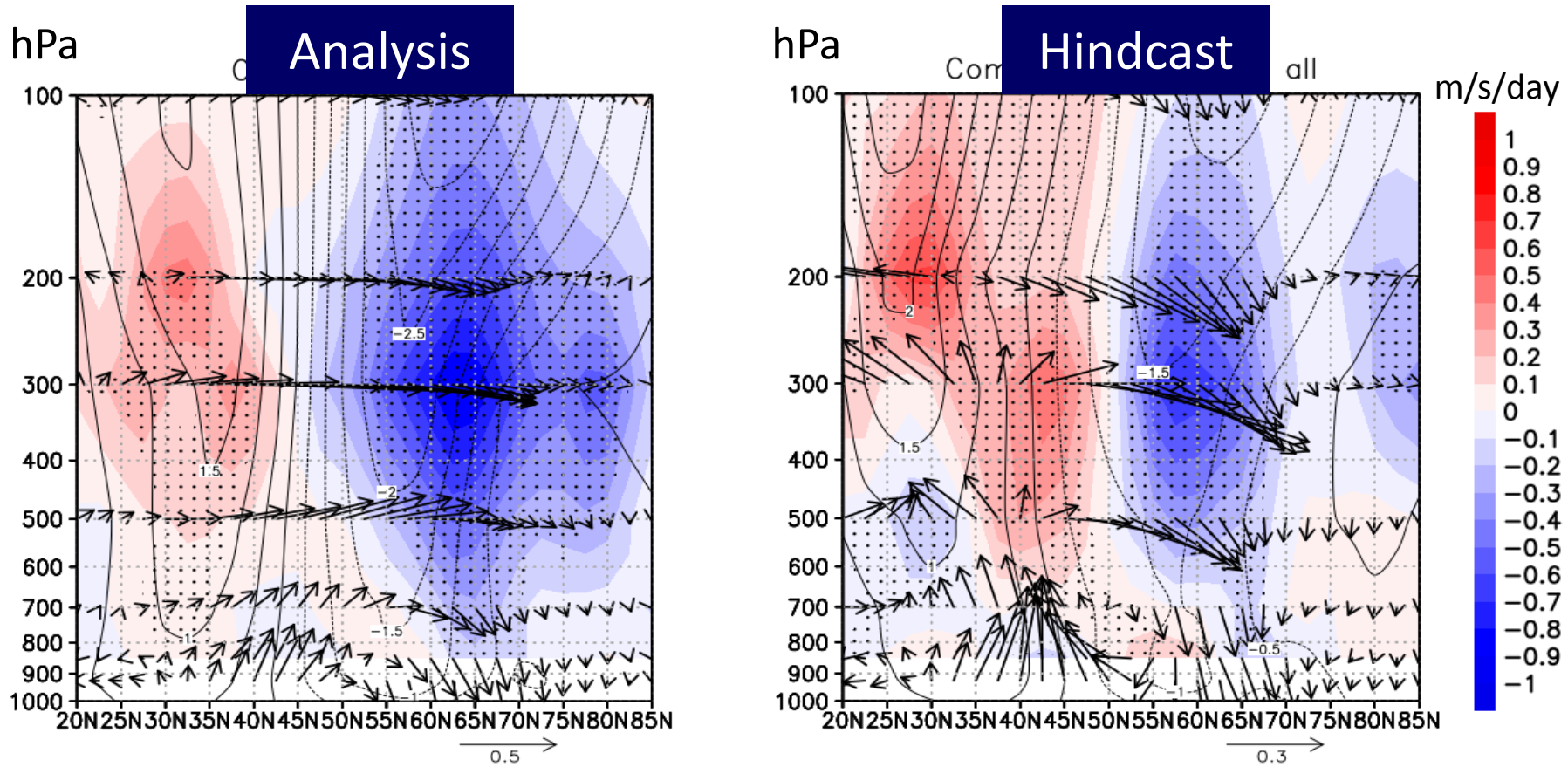
3.4 Zonal mean wind anomaly (Negative phases)



Composite of the zonal mean wind anomaly (28-day averaged) for the cases initiated in the negative phases. Contour shows the zonal mean wind and shading shows its anomaly.

- Equatorward shift of the westerly jet is the characteristic of the negative phases of the AO.
- One-month EPS simulated the anomaly field very well.

3.5 Wave-mean flow interaction (Negative cases)

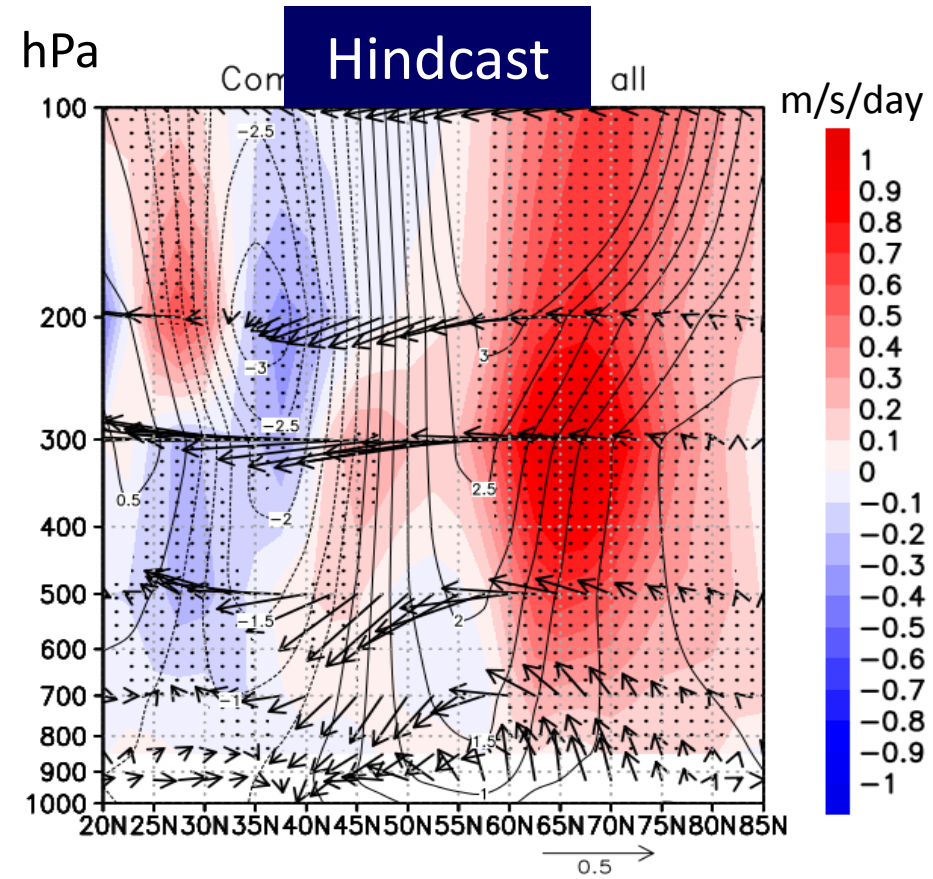
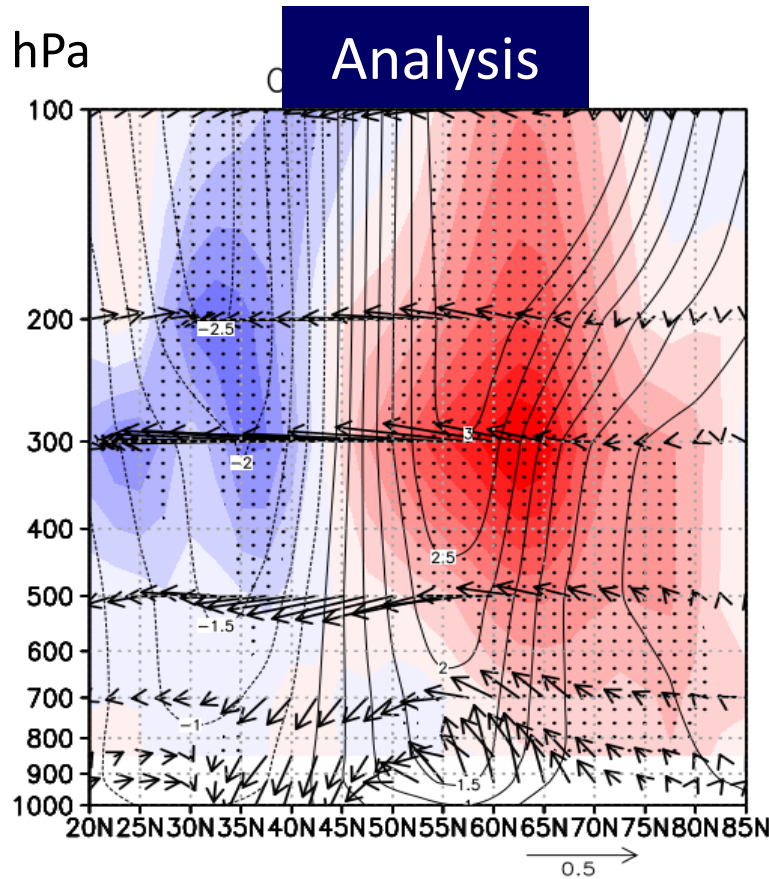


Composite of EP flux anomaly (28-day averaged) . Vectors show EP flux anomaly and shading shows its divergence for all wave numbers. Dotted area indicate statistical significance of EP flux anomaly at 90% level by Student's t-test. Contour shows composite of zonal mean wind anomaly.

- Negative phases of the AO is enforced by eddies.
- One-month EPS simulated the pattern of convergence and divergence of EP flux anomaly.

3.6 Wave-mean flow interaction (Positive cases)

hPa

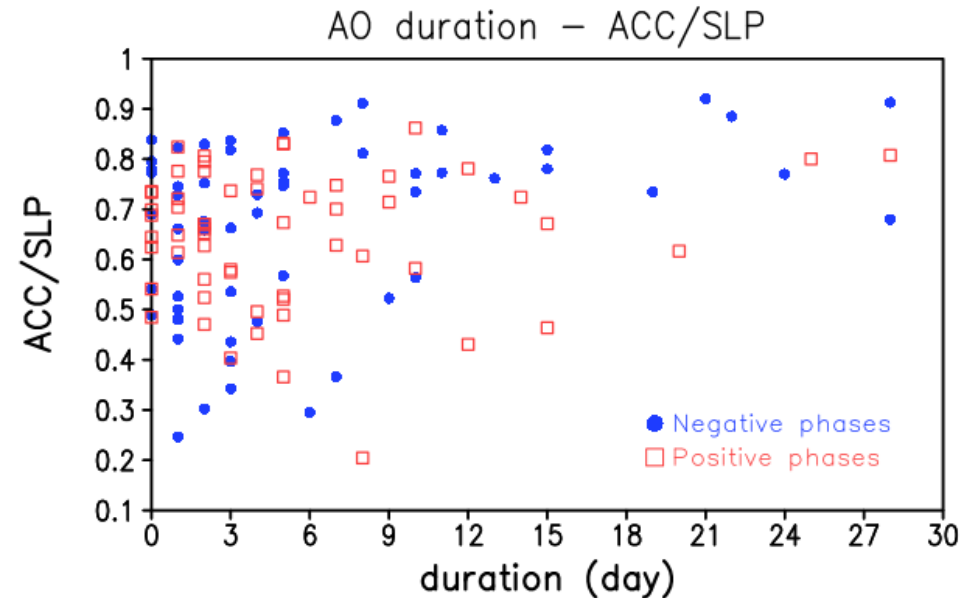
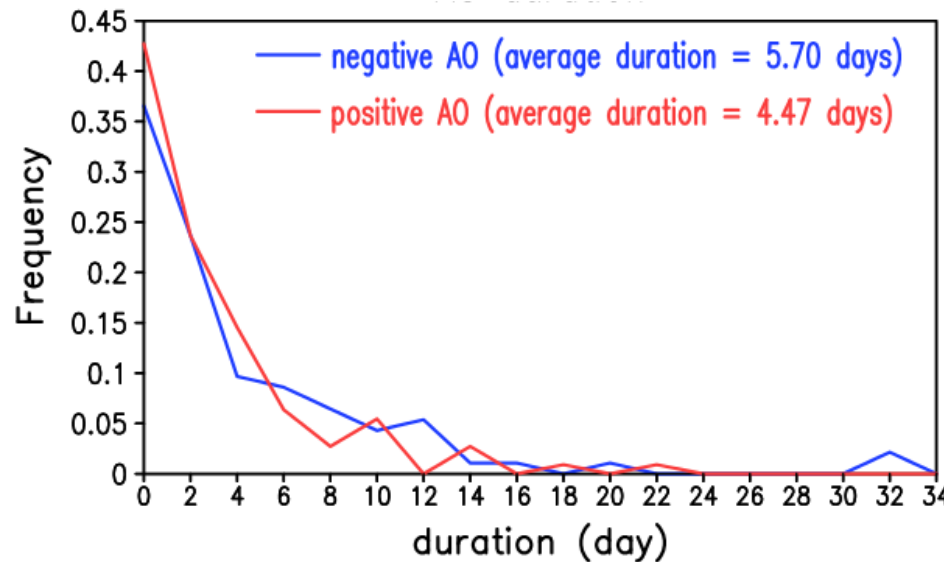


Composite of EP flux anomaly (28-day averaged) . Vectors show EP flux anomaly and shading shows its divergence of all wave numbers. Dotted area indicate statistical significance of EP flux anomaly at 90% level by Student's t-test. Contour shows composite of zonal mean wind anomaly.

- The dynamical process works for the positive cases as the negative cases.
- One-month EPS also simulated the pattern of convergence and divergence of EP flux anomaly.

3.7 Discussions

- Why negative phase events is more predictable than the positive cases?



- The difference between negative and positive phases of the AO is ..
 - The duration of negative AO is longer than positive one.
- Besides, one-month EPS tends to simulate well if the same phase lasts longer.

4. Summary

- Relationship between AO and predictability in subseasonal time scale was investigated using hindcast of the latest JMA's one-month EPS.
 - Prediction skills initiated in the negative phases of the AO were higher than that in other phases for about 3 weeks from the initial.
- Dynamical process serving the predictability initiated in the negative phases was investigated.
 - Westerly jet was shifted equatorward associated negative phases of the AO and it was enforced by the eddies mean-flow interaction.
 - One-month EPS simulated the characteristics well.

Thank you for your attention!

➤ References

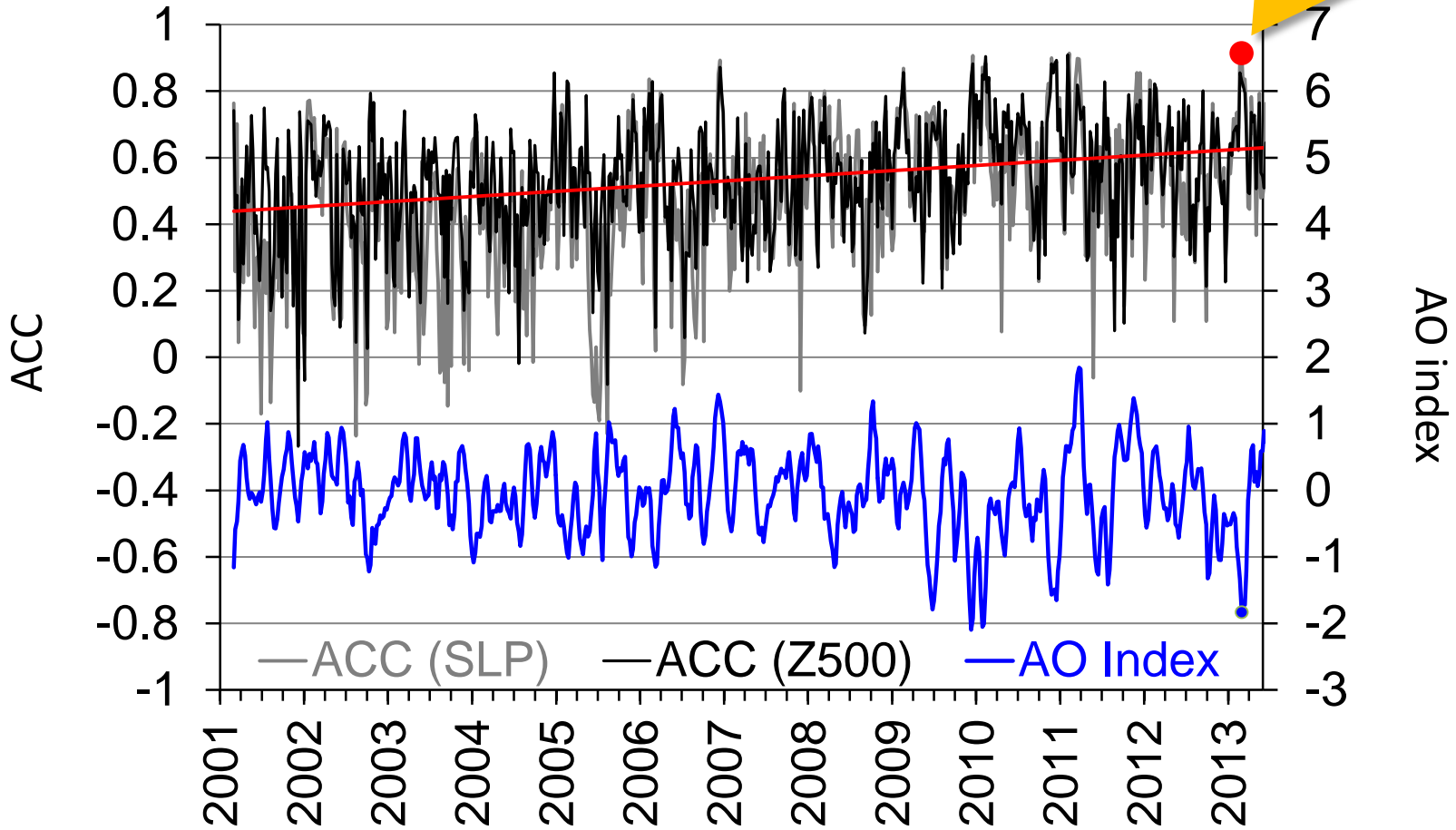
- Buizza, R., Miller, M., and Palmer, T.N., 1999: Stochastic simulation of model uncertainties. *Q.J.R. Meteorol. Soc.*, **125**, 2887-2908.
- Jung, T., M. J. Miller, T. N. Palmer, P. Towers, N. Wedi, D. Achuthavarier, J. M. Adams, E. L. Altshuler, B. A. Cash, J. K. Kinter III, L. Marx, C. Stan, and K. I. Hodges, 2012: High-resolution global climate simulations with the ECMWF model in Project Athena: Experimental design, model climate and seasonal forecast skill. *J. Climate*, **25**, 3155-3172.
- Lorenz, D. J., and D. L. Hartmann, 2003: Eddy-zonal flow feedback in the Northern Hemisphere winter. *J. Climate*, **16**, 1212-1227.
- Sugimoto, H., and Y. Takaya, 2013: A method of predicting sea ice boundary conditions for the One-month Ensemble Prediction System. WGNE Blue Book.
- Thompson, D. W. J, and J. M. Wallace, 1998: The Arctic Oscillation signature in the wintertime geopotential height and temperature fields. *Geophys. Res. Lett.*, **25**, 1297-1300.

➤ Future works

- Since we focused on only tropospheric dynamics in this study, we should investigate the contribution of another factors such as stratosphere, ENSO, MJO, and Arctic sea ice which are also thought to be important for AO variability.
 - Especially, since sea ice distribution was well predicted in the One-month EPS used in this study, we may be able to obtain some implications.

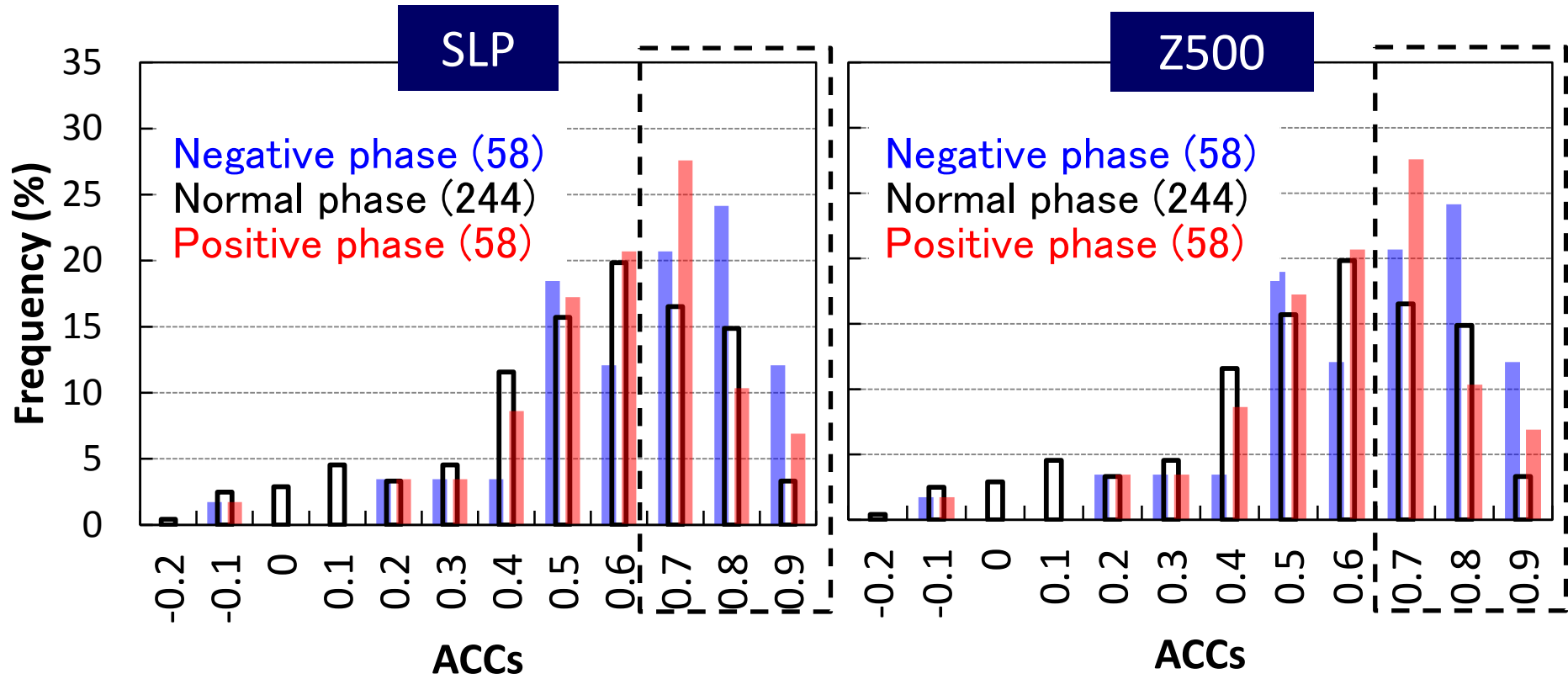
➤ AO and its prediction skills

March 2013
ACC/SLP: **0.914**



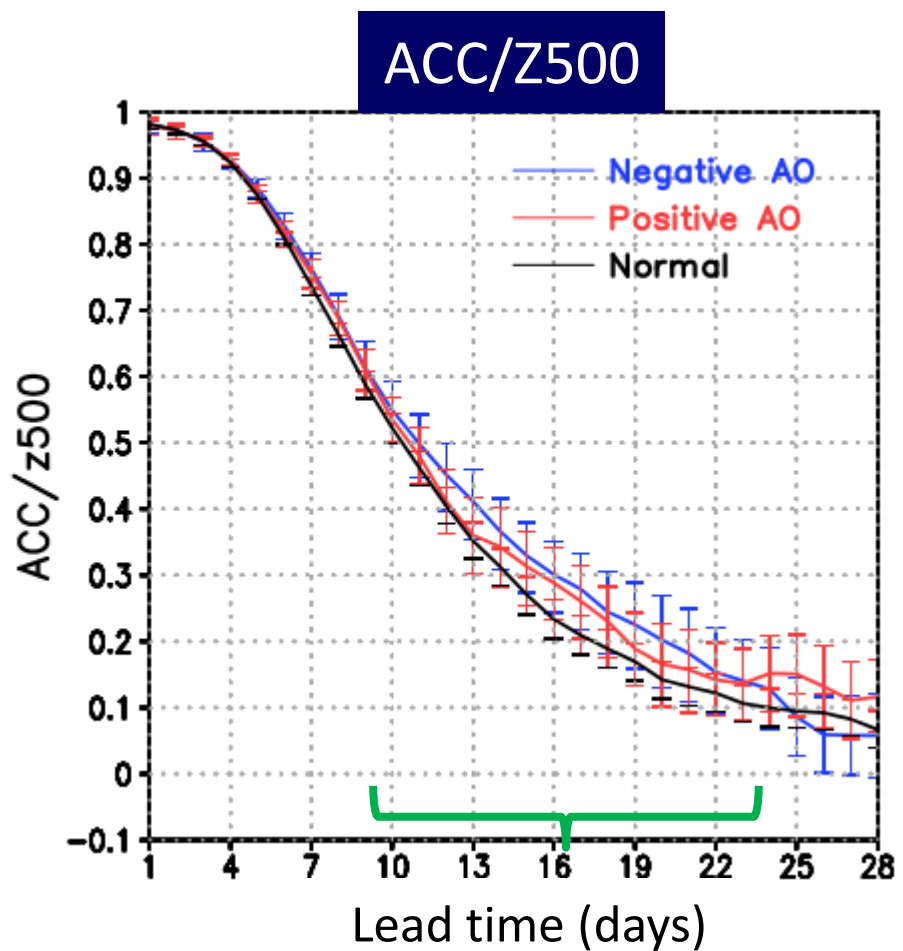
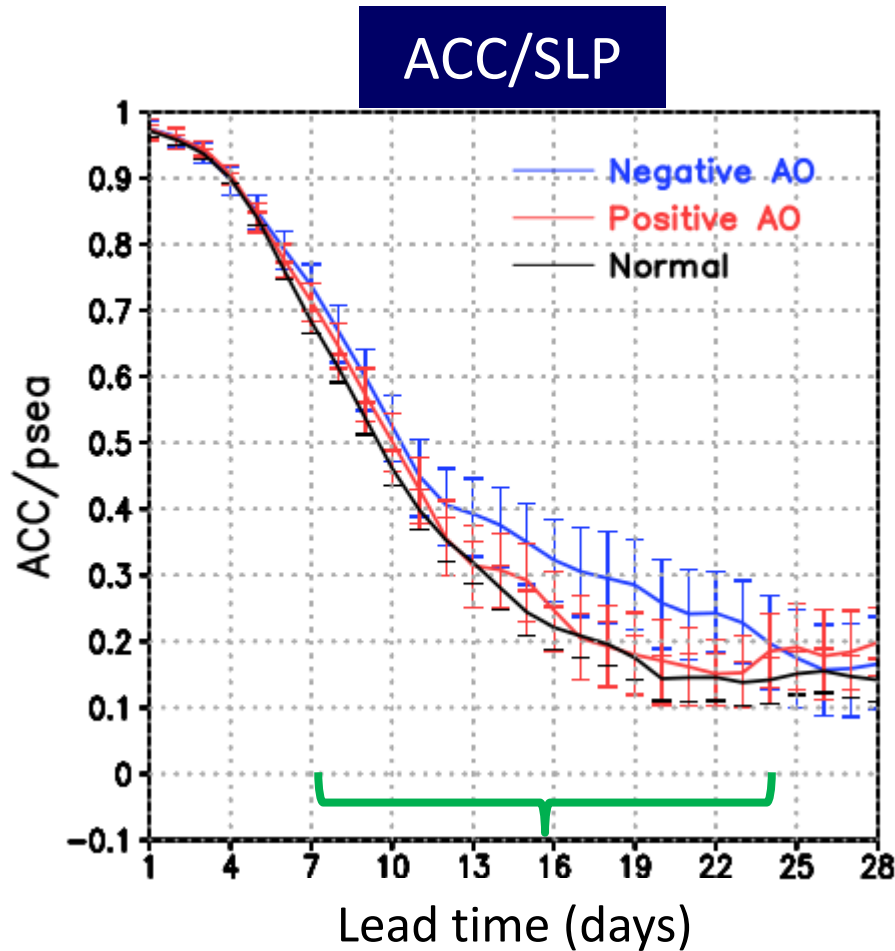
AO index and ACC of operational JMA's One-month Ensemble Prediction System (One-month EPS) . ACC is calculated by the 28-day averaged prediction field.

➤ Prediction skill for each phase event



- Negative phase events tend to record higher prediction skills than other phase events.
- A rate of ACCs above 0.7 for SLP (Z500) in negative phases is roughly 25% (15%) higher than that for normal phases.

➤ Prediction skill for each lead time

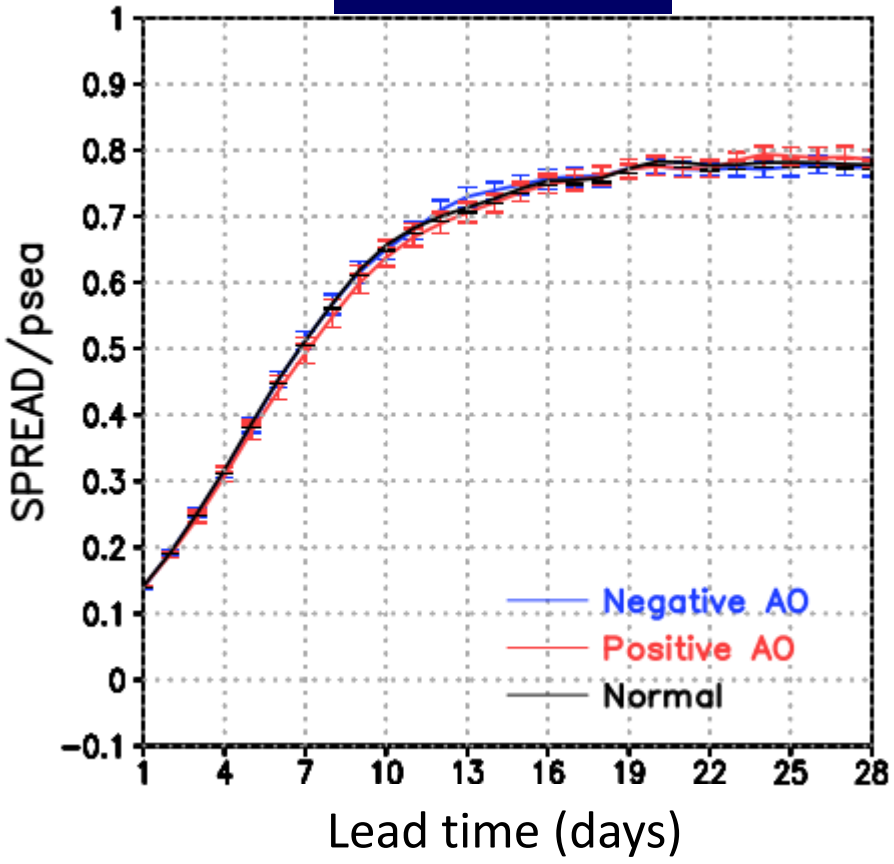


Error bar shows the 95% confidence level calculated by 1000 subsamples generated with the bootstrap method.

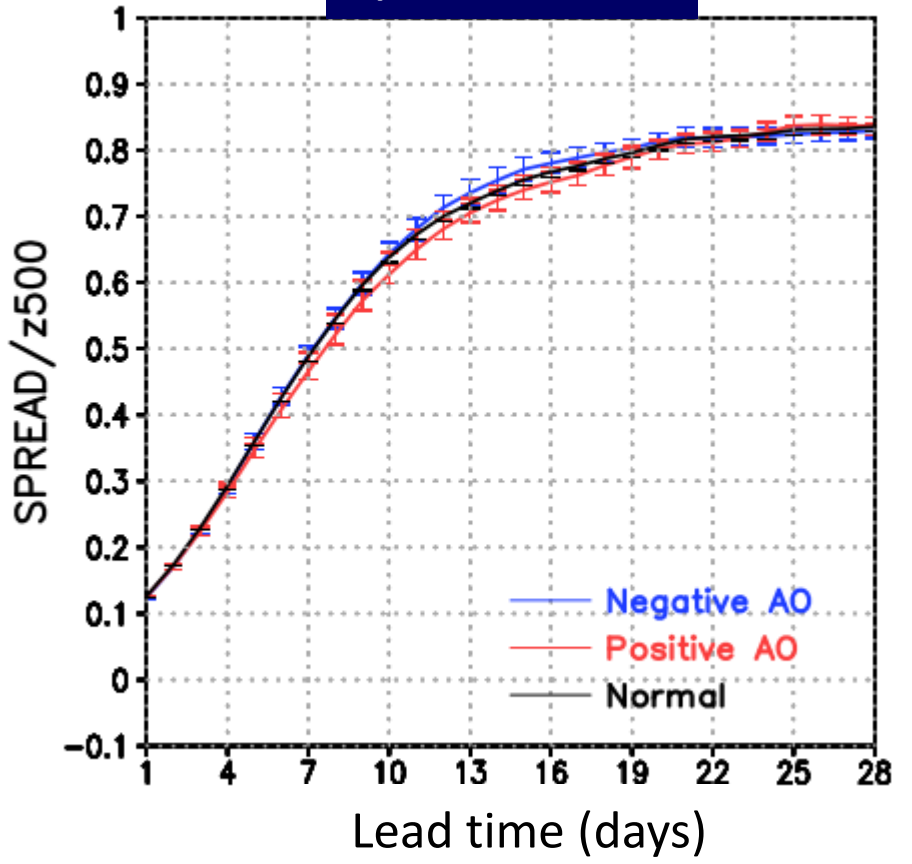
- ACCs initiated in negative phases are higher than that in normal phases for almost all forecast times.

➤ Spread

spread/SLP

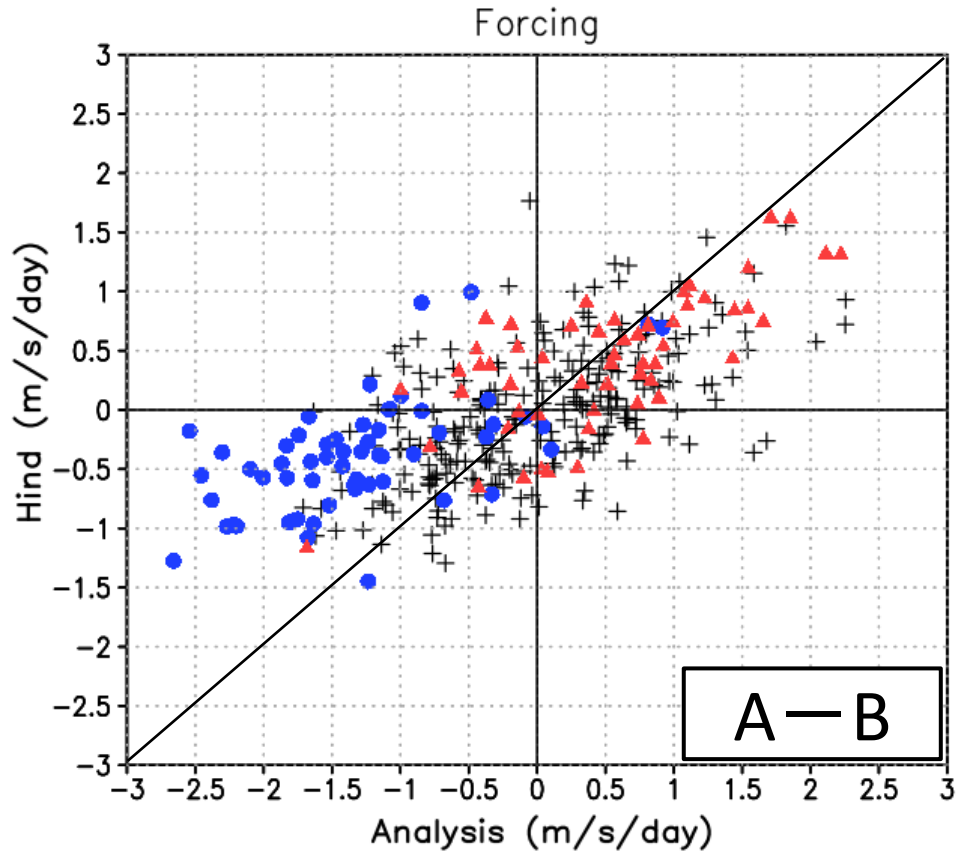
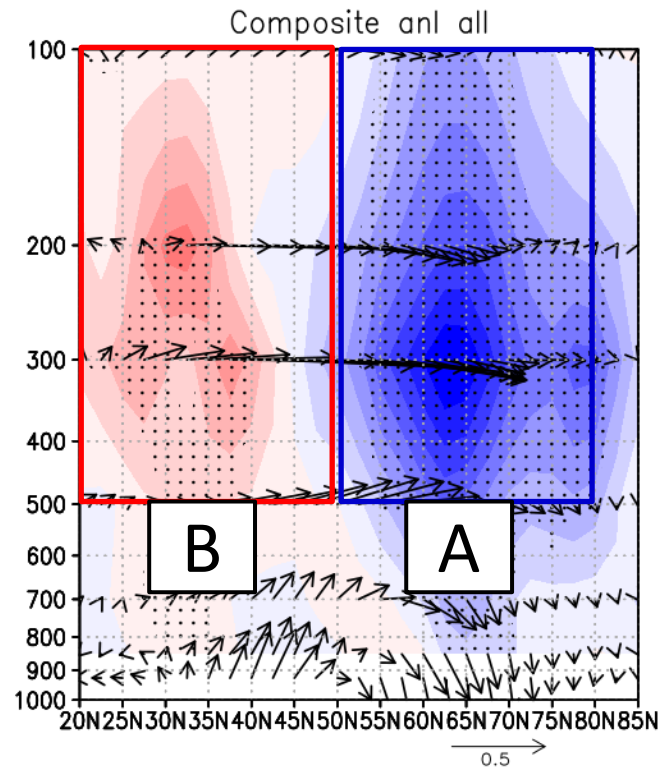


spread/Z500

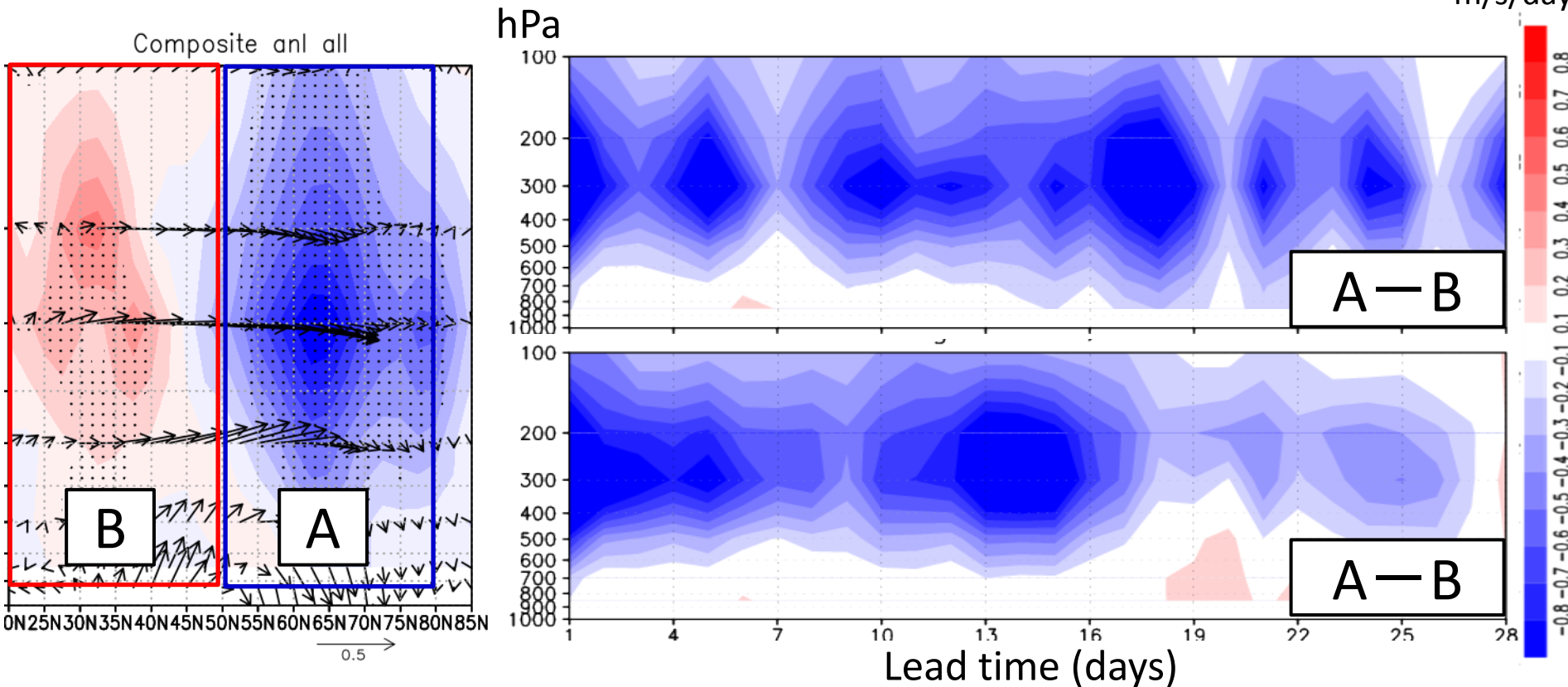


Spread averaged over Northern hemisphere is shown. Error bar shows the 95% confidence level calculated by 1000 subsamples generated with the bootstrap method.

➤ Eddy forcing



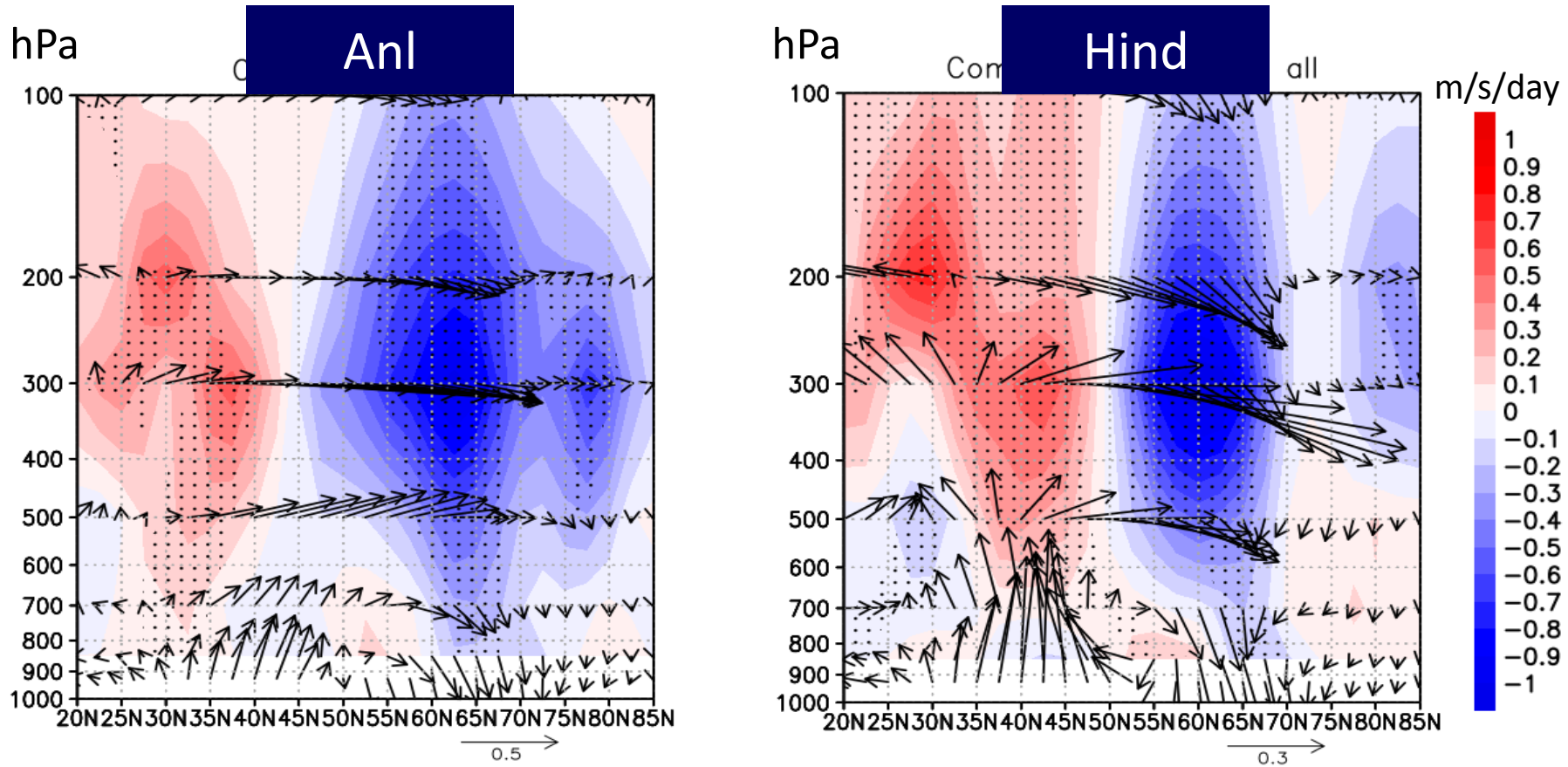
➤ Wave-mean flow interaction (Negative cases)



Composite of the difference of EP-flux convergences anomaly for all wave numbers. Blue shading means that eddies enforced to shift the westerly jet equatorward.

- Westerly jet is enforced to shift equatorward by the eddies for about one month from the initial day.
- Though there are slight difference between the analysis and prediction, westerly jet is also enforced to shift equatorward by eddies in the prediction of the one-month EPS.

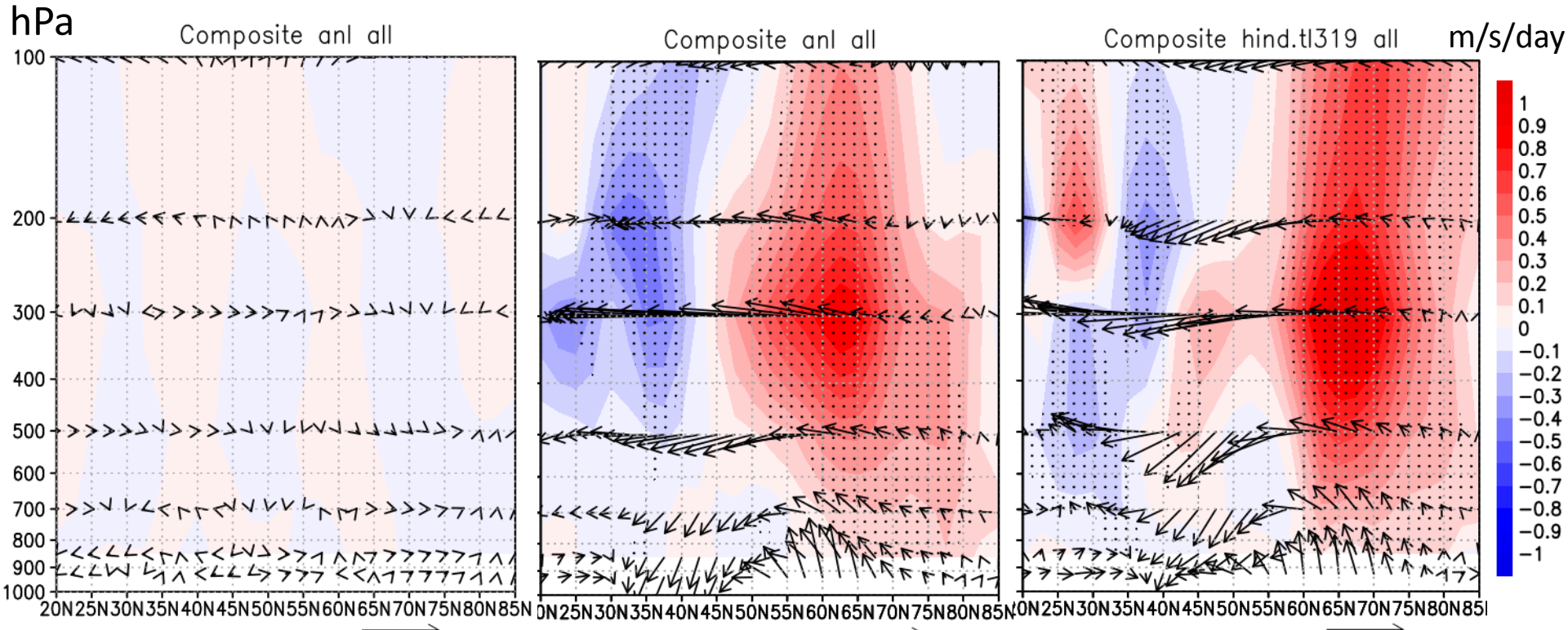
➤ Wave-mean flow interaction (-1.5σ)



Composite of EP flux anomaly (28-day averaged) . Vectors show EP flux anomaly and shading shows its divergence of all wave numbers. Dotted area indicate statistical significance of EP flux anomaly at 90% level by Student's t-test. Contour shows composite of zonal mean wind anomaly.

- Negative phases of the AO is enforced by eddies.
- One-month EPS simulated the pattern of convergence and divergence of EP flux anomaly.

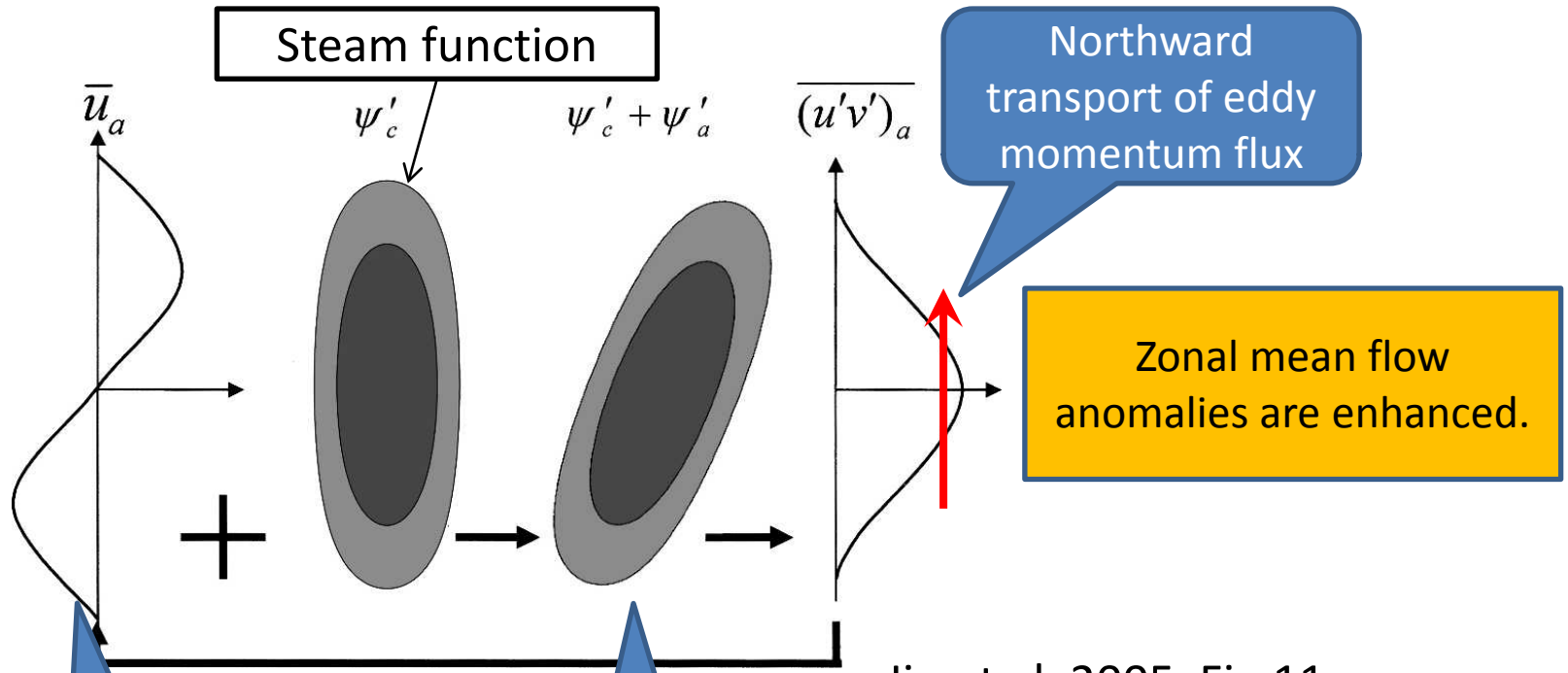
Wave-mean flow interaction (Positive cases)



Composite analysis of EP flux anomaly. Vectors show EP flux anomaly and shading shows its divergence. Dotted area indicate statistical significance at 90% level by Student's t-test..

➤ Eddy feedback mechanism

Tilted-trough mechanism (Kimoto et al. 2001) is a concept of positive eddy-mean flow interaction.



Jin et al. 2005, Fig.11

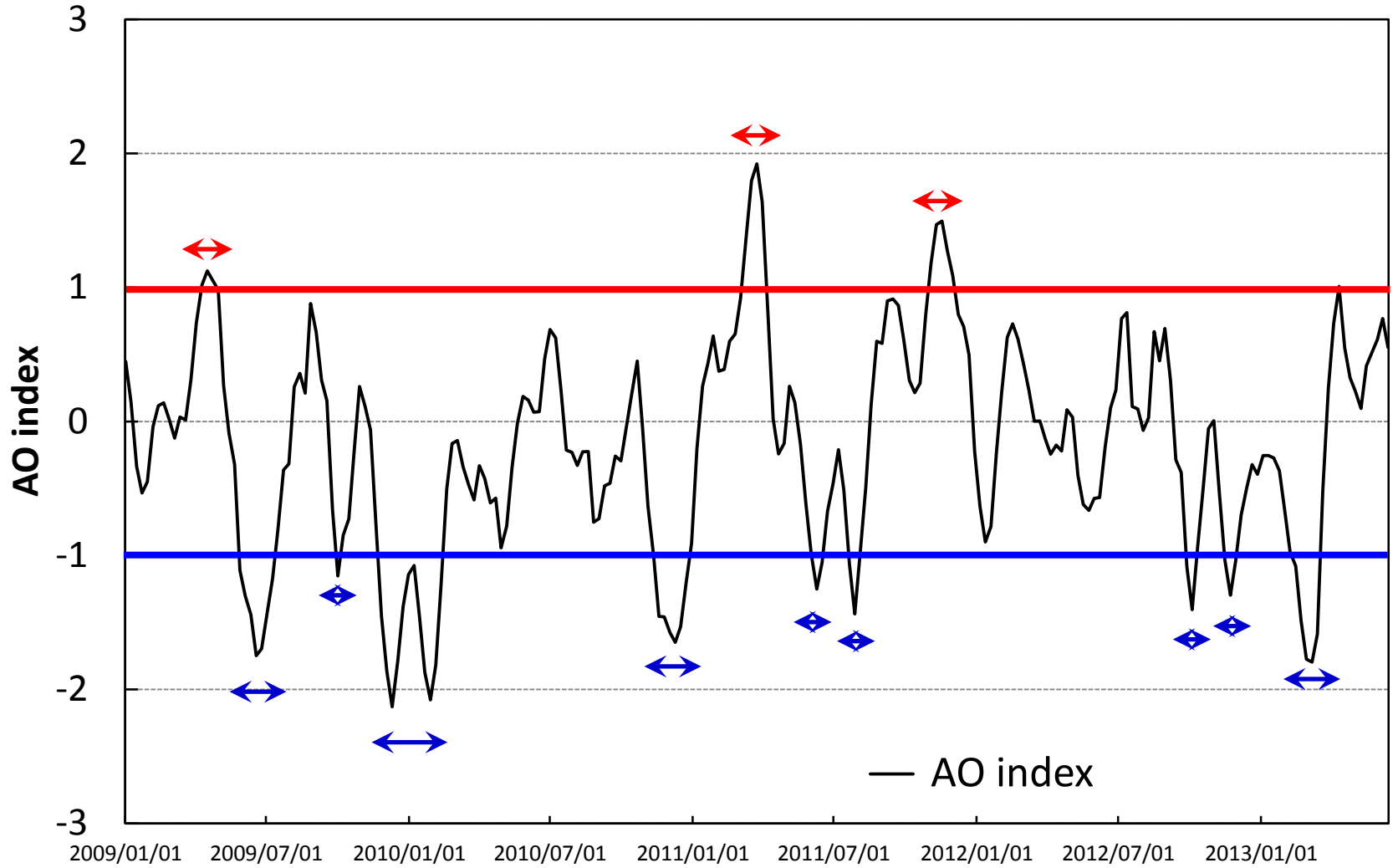
Zonal mean flow anomalies associated AO

Trough tilted NE-SW direction

Northward transport of eddy momentum flux

Zonal mean flow anomalies are enhanced.

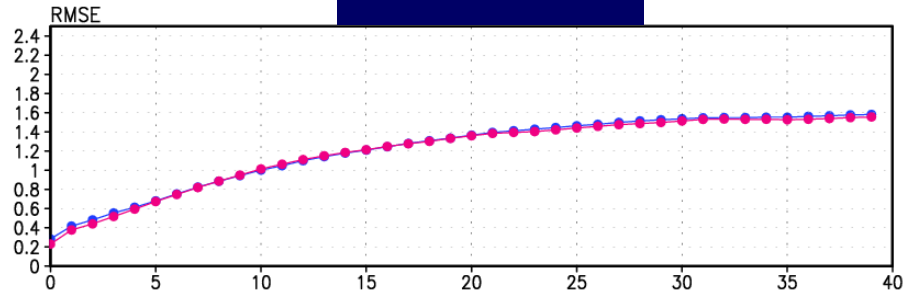
➤ Duration of AO events



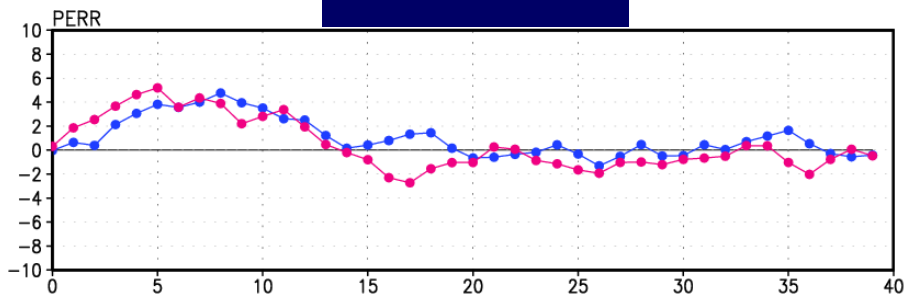
➤ Prediction skill of the MJO

MJO index 1981–2010

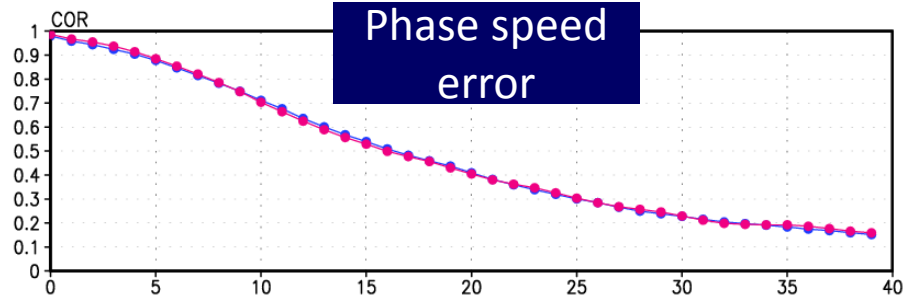
RMSE



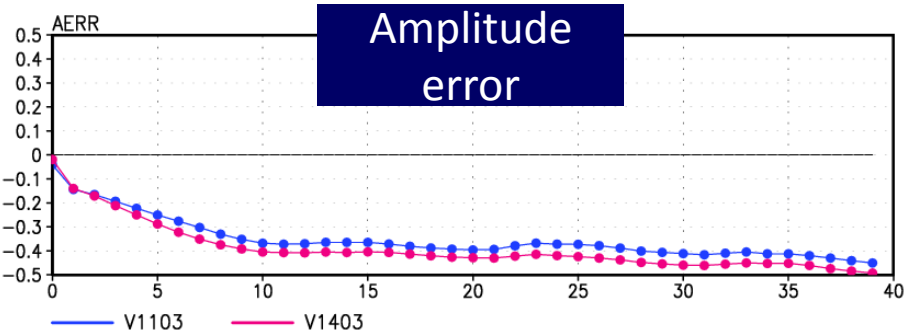
Phase error



Phase speed error

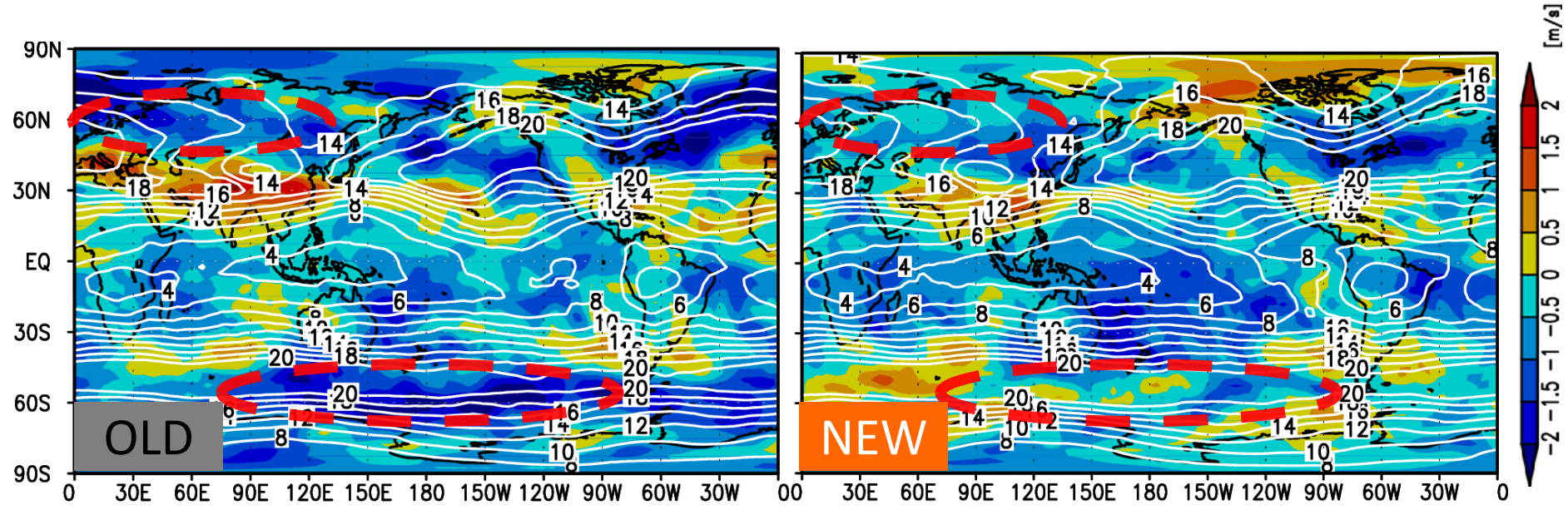


Amplitude error



- Unfortunately, prediction skill of MJO was not improved.

➤ High frequency eddy activities



Bias of the high frequency eddy activity $\sqrt{u'^2 + v'^2}$ at 300 hPa in January.

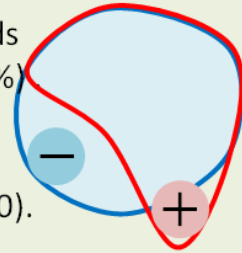
Contour shows monthly averaged prediction and shading shows its bias. High frequency eddy was extracted by using 2nd butter-worth filter (cut off: 10days) . Here, and mean eddy component of zonal and meridional wind respectively.

➤ A method of sea ice estimation

Initial (t = 0)

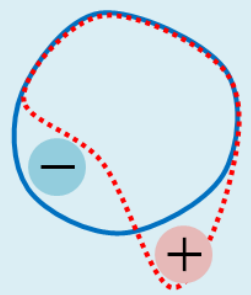
Step 1. Classification of ocean grids : sea ice grids ($SIC(x,y,t) \geq 55\%$) and open-sea grids ($SIC(x,y,t) < 55\%$)

Step 2. Calculation of $SICa(x,y,0)$ and $SIEa(h,0)$:
 $SICa(x,y,0) = SIC(x,y,0) - SICc(x,y,0)$, $SIEa(h,0) = SIE(h,0) - SIEc(h,0)$.



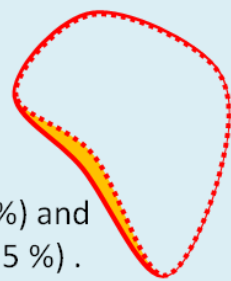
Blue line : climatological sea ice edge
 Red line : initial sea ice edge
 Signs of + and - : regions where $SICa$ are positive and negative .

Lead time of less than 14 days (t ≤ 14) < Combination of persistent initial SICa and initial SIEa >



Step 3. Prediction of $SIC(x,y,t)$:
 $SIC(x,y,t) = SICa(x,y,0) + SICc(x,y,t)$.

Step 4. Classification of ocean grids : potential sea ice grids ($SIC(x,y,t) \geq 55\%$) and potential open-sea grids ($SIC(x,y,t) < 55\%$) .



Step 5. Adjustment of the potential sea ice distribution : modifying the potential sea ice (open-sea) grids with lower (higher) climatological frequency to open-sea (sea ice) grids to satisfy
 $SIEa(h,t) = SIEa(h,0)$,
 where $SIEa(h,t) = SIE(h,t) - SIEc(h,t)$.

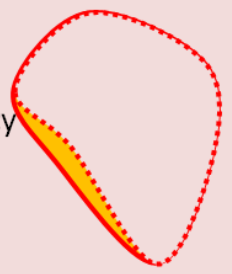
Red broken line : potential sea ice edge

Red solid line : estimated sea ice edge
 Orange shaded area : added sea ice area

Iterations from Step 3 to Step 5

Lead time of more than 15 days (t ≥ 15) < Persistent initial SIEa >

Step 6. Adjustment of the previous day's sea ice distribution : modifying the previous sea ice (open-sea) grids with lower (higher) climatological frequency to open-sea (sea ice) grids to satisfy
 $SIEa(h,t) = SIEa(h,0)$,
 where $SIEa(h,t) = SIE(h,t) - SIEc(h,t)$.



Red broken line : sea ice edge in the previous day
 Red solid line : estimated sea ice edge
 Orange shaded area : added sea ice area

Iterations of Step 6

* $SICa$: SIC anomalies, $SICc$: SIC climatologies, $SIEa$: SIE anomalies, $SIEc$: SIE climatologies
 (x, y) : horizontal position, t : lead time [day], h : northern or southern hemisphere